

Mirrorless parametric oscillation in an atomic Raman processKai Zhang,¹ Jinxian Guo,¹ Chun-Hua Yuan,¹ L. Q. Chen,^{1,*} Chengling Bian,¹ Bing Chen,¹ Z. Y. Ou,^{1,2,†} and Weiping Zhang^{1,‡}¹*Quantum Institute for Light and Atoms, State Key Laboratory of Precision Spectroscopy, Department of Physics, East China Normal University, Shanghai 200062, P. R. China*²*Department of Physics, Indiana University–Purdue University Indianapolis, 402 N. Blackford Street, Indianapolis, Indiana 46202, USA*

(Received 10 April 2014; published 27 June 2014)

We investigate experimentally and theoretically the onset of parametric oscillation in a single-pass atomic Raman scattering process without the optical feedback. We find that this Raman oscillation effect is due to the coherent buildup of the atomic spin waves, and therefore the threshold of the Raman pump power for the onset of the oscillation depends on the decoherence time of the atomic spin waves and the Raman coupling constant but is not sensitive to the loss of the Stokes field, unlike the effect of amplified spontaneous emission. A simple theory of atomic Raman process fits the experimental results very well. The long decoherence time of the atomic spin waves in the atomic Raman process leads to a threshold power as low as a few hundred microwatts.

DOI: [10.1103/PhysRevA.89.063826](https://doi.org/10.1103/PhysRevA.89.063826)

PACS number(s): 42.65.Dr, 42.50.Gy, 42.50.Ct, 32.80.Qk

I. INTRODUCTION

Stimulated Raman scattering was one of the nonlinear optical effects discovered soon after the invention of laser in the early 1960s [1]. Theoretical descriptions [2] basically provided only some gain mechanisms and attributed the observed sharp onset of the coherent Raman oscillation to the optical feedback due to Rayleigh scattering of the Raman fields or diffusive reflection of the window of sample cells [3], similar to the mechanism of the laser's operation. More complicated self-focusing theory is successful in some cases [4]. But attention was quickly shifted to the applications of stimulated Raman scattering in many different fields [5]. There was no further detailed study of the quantitative interpretation of the onset of Raman oscillation because of the belief in the difficulty of characterizing those optical feedbacks.

Recently study of Raman scattering has been focused on atomic systems with metastable energy levels, such as alkaline atoms and some rare earth ions [6–8]. The long lifetime of these energy levels is ideal for storage of quantum information [9–14] and for quantum memory [15,16]. In the Raman scattering process with atoms, the coupling between the light and atoms provides a three-wave mixing mechanism [17,18] for the Raman pump field, the scattered Stokes field, and a collective atomic excitation wave, known as the atomic spin wave. There has been research into the temporal and spatial behaviors of the Stokes field and atomic spin wave [7,8]. The existence of the atomic spin waves as real objects can be confirmed indirectly by reading them out via another process [19].

It was recently discovered [20–24] that Raman conversion efficiency in an atomic medium can be greatly enhanced with the help of the atomic spin waves. The underlining physics is that when the pump field is strong, the three-wave mixing process is an amplification process [23] for both the Stokes field and the atomic spin wave with the Raman gain

depending on the strength of the Raman pump field. The role of the atomic spin wave is to act like a seed to the Raman amplification [22], leading to a stimulated Raman process. Note that the seed is not from the Stokes field, as is usually done, but from the atomic excitations. Even so, the effect is the same: greatly enhanced Raman conversion efficiency. Good Raman conversion efficiency can be achieved in a wide range of Raman pump power, even down to the single-photon level in principle [25].

All the phenomena mentioned above are possible because of the long lifetime of the atomic spin wave, which is on the order of microseconds [19,26,27] in some cases and even a few seconds [28,29] in others. Furthermore, coherent stimulated Raman emission occurs at a pump power as low as a few hundreds of microwatts [24], as compared to megawatts in other systems such as molecular gases [30]. This leads us to wonder what makes the threshold so low for the onset of the stimulated Raman scattering. In this paper we investigate in detail the onset of the Raman oscillation in an atomic vapor cell. We study how laser detuning and decoherence time of the atomic spin wave affect the onset threshold. We find that the onset of the Raman oscillation is not due to optical feedback, as commonly believed [3,5,31,32], but is from the coherent buildup of the atomic spin wave. Therefore there is no need for optical feedback.

It should be noted that this is a genuine mirrorless laser operation where no optical feedback exists. In general, mirrorless laser operation often refers to laser operation without the need for a mirror, but in most cases some kind of optical feedback exists to give rise to a threshold for the laser oscillation to generate a coherent optical field [33,34]. However, genuine mirrorless laser operations without any optical feedback do occur and usually deal with single-pass traveling wave for the generated coherent field [35–37]. Because of the single-pass nature in these effects, a strong pump is required and is often in pulsed form in order to prepare the active medium for the buildup of the coherent emission. Genuine mirrorless laser operation in Raman processes takes the form of amplified spontaneous emission where the transition from the regime of spontaneous thermal radiation to the regime of coherent stimulated emission occurs as the strong Raman pump intensity

*lqchen@phy.ecnu.edu.cn

†zou@iupui.edu

‡wpzhang@phy.ecnu.edu.cn

increases [38]. This is possible because of the good Raman gains obtained under the strong pulsed Raman pump field. On the other hand, the phenomenon in our experiment has a completely different mechanism. Henceforth, the threshold effect occurs at a pump power level as low as a few hundred microwatts, which is attributed to the long decoherence time of the atomic spin wave in the cell and is independent of the loss of the Stokes field.

II. EXPERIMENTAL PROCEDURE AND RESULTS

The experimental setup is shown in Fig. 1(a). The protocol is based on a Raman process in a ^{87}Rb atomic ensemble. The pure ^{87}Rb atoms are contained in a 50 mm-long glass cell. The cell is placed inside a four-layer μ -magnetic shielding to reduce stray magnetic fields and is heated up 68 °C using a bifilar resistive heater. The energy levels of ^{87}Rb atom and time sequence are given in Figs. 1(b) and 1(c) together with laser frequencies. The lower two energy states $|g\rangle$ and $|m\rangle$ are the hyperfine split ground states $^2S_{1/2}$ ($F = 1, 2$) with a frequency difference of 6.87 GHz, and the three higher energy states $|e_1\rangle$, $|e_2\rangle$, and $|e_3\rangle$ are the excited states ($|5^2P_{1/2}, F = 1, 2\rangle, |5^2P_{3/2}\rangle$). An optical pumping field (OP, not shown) is turned on for 90 μs and resonant with the transition of $|m\rangle \rightarrow |e_3\rangle$ to prepare the atoms in the $|g\rangle$ state. After the OP pulse, a Raman pump pulse P is turned on for 0.5 μs . It couples the state $|e_1\rangle$ or $|e_2\rangle$ with $|g\rangle$ and generates a Stokes field S and the corresponding atomic spin wave S_a . The atomic spin wave stays in the cell, and the Stokes field travels out together with the pump field. The Stokes field can be separated from the pump field by a polarization beam splitter because their polarizations are orthogonal to each other and detected by a photodetector. Then a read field is sent in to read out the atomic spin wave [19]: when the atomic spin wave is nonzero, the read field will produce an anti-Stokes field (AS) that can be detected by another detector. The strength of the AS field is proportional to the size of the atomic spin wave.

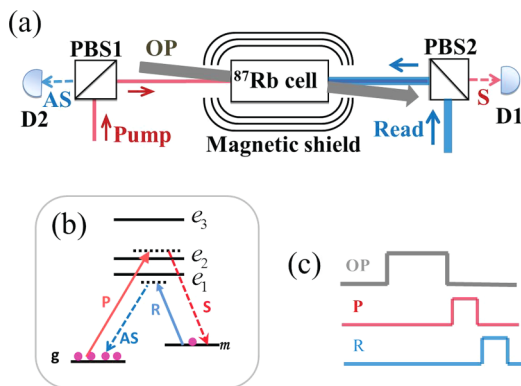


FIG. 1. (Color online) (a) Experimental arrangement. PBS: polarized beam splitter; D1, D2: photodetector; OP: optical pump pulse; S: Stokes field; AS: anti-Stokes. (b) Energy levels of ^{87}Rb for Raman scattering; $|g\rangle$ and $|m\rangle$ are the hyperfine split ground states $|5^2S_{1/2}, F = 1, 2\rangle$; $|e_1\rangle = |5^2P_{1/2}, F = 1\rangle$, $|e_2\rangle = |5^2P_{1/2}, F = 2\rangle$, and $|e_3\rangle = |5^2P_{3/2}\rangle$. (c) Timing sequence. R: read pulse; P: pump pulse.

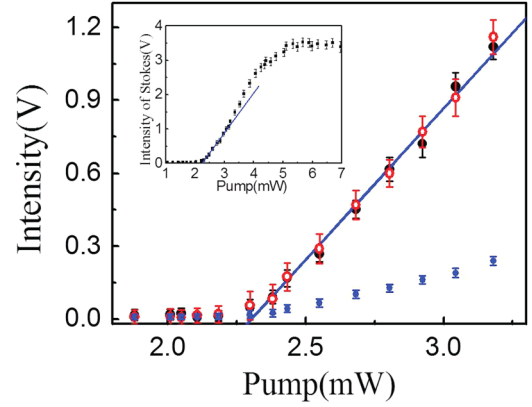


FIG. 2. (Color online) Output anti-Stokes and Stokes fields as a function of the Raman pump power, showing a laser-like threshold. Black dot: Stokes light; blue dot: anti-Stokes light; red circle: anti-Stokes times five. Inset: Saturation regime is shown for higher Raman pump power.

The intensity of the anti-Stokes field as well as the Stokes field is recorded when the power of the pump field (P_p) is changed from about 100 μW to a few milliwatts while other experimental conditions (such as detuning and temperature) are fixed. One typical experimental sample is shown in Fig. 2 when the detuning is $\Delta = 0.8$ GHz. Both the observed intensities exhibit a sharp kink when P_p is equal to 2.3 mW. The sharp kink is typical of a laserlike threshold effect. Thus, we observe an onset of a mirrorless oscillation phenomenon in the Raman process for both the atomic spin wave and the Stokes field. The atomic spin wave and the Stokes field are equal to zero below threshold, i.e., 2.3 mW. Above the threshold, the atomic spin wave and the Stokes field increase linearly with P_p . The threshold power of the Raman pump field, labeled P_{th} , can be extracted as the x -axis intercept of the linear fit of the data above the threshold.

In the inset of Fig. 2, we show the saturation regime when the power of the pump field P_p increases further. In the present paper, we focus on the linear growth regime to study the threshold effect. In our previous paper [24], we worked in the saturation regime where the conversion efficiency is high. Another difference between present work and previous paper [24] is the optical feedback effect. In present paper, there is not optical feedback effect, the pump field just passes through the cell once. In the previous paper, there are optical feedback effects, and the pump field traverses the cell twice by adding a reflecting mirror at the end of the cell.

III. THEORETICAL EXPLANATION

To understand the laserlike threshold effect shown in Fig. 2, we recall that the Raman process in an atomic ensemble of N_a atoms with an energy level diagram as shown in Fig. 1(b) is basically a three-wave mixing process, where besides the Raman pump and the Stokes fields, the third field is the atomic coherence described by a quantum field operator $\hat{S}_a \equiv (1/\sqrt{N_a}) \sum_i |g\rangle_i \langle m|$. In a simplified one-dimensional traveling wave model and under the condition of a strong and undepleted classical pump field A_p , the coupled equations for

the Stokes quantum field \hat{a}_S and the atomic spin wave \hat{S}_a are given by [23,39,40]

$$\left(\frac{\partial}{\partial t} + c\frac{\partial}{\partial z}\right)\hat{a}_S(z,t) = i\eta A_P G(z)\hat{S}_a^\dagger(z,t), \quad (1)$$

$$\frac{\partial}{\partial t}\hat{S}_a(z,t) = -\Gamma_a\hat{S}_a + i\eta A_P G(z)\hat{a}_S^\dagger(z,t) + \hat{F}(z,t), \quad (2)$$

where $\eta \equiv \sqrt{N_a}g_{eg}g_{em}/\Delta$ with g_{eg}, g_{em} as the coupling coefficients between the excited state and the lower level states. Δ is the detuning from the excited state $|e\rangle$ for both the Stokes and Raman pump fields, which satisfy the two-photon resonance condition: $\omega_P - \omega_S = \omega_{mg}$. $G(z)$ is the spatial mode function for the pump field, Γ_a is the decoherence coefficient of the atomic spin wave, and \hat{F} is the Langevin quantum noise operator. Notice that Eq. (1) for the change of the Stokes field is a propagation equation, reflecting the fact that the Stokes field is a single-pass traveling field without feedback. On the other hand, Eq. (2) describes the time evolution of the atomic spin wave, which stays inside the atomic medium and does not travel outside.

Making a change of variables: $\zeta = z, \tau = t - z/c$, we transform into the traveling frame and take the classical average of the Stokes field $a_S = \langle \hat{a}_S \rangle$ and the atomic spin wave $S_a = \langle \hat{S}_a \rangle$. Then Eqs. (1) and (2) are changed to

$$c\frac{\partial}{\partial \zeta}a_S(\zeta, \tau) = i\eta A_P G(\zeta)S_a^*(\zeta, \tau), \quad (3)$$

$$\frac{\partial}{\partial \tau}S_a(\zeta, \tau) = -\Gamma_a S_a(\zeta, \tau) + i\eta A_P G(\zeta)a_S^*(\zeta, \tau). \quad (4)$$

Next, we assume both the Stokes and the atomic spin wave are in some single spatial mode so that we can separate the space and time parts of the fields: $a_S(\zeta, \tau) = A_S(\tau)\varphi(\zeta)$, $S_a(\zeta, \tau) = S_a(\tau)\psi(\zeta)$. After writing space and time parts separately, Eqs. (3) and (4) are changed to

$$c\alpha_1\frac{d\varphi(\zeta)}{d\zeta} = G(\zeta)\psi^*(\zeta), \quad (5)$$

$$\alpha_2\psi(\zeta) = G(\zeta)\varphi^*(\zeta), \quad (6)$$

$$A_S(\tau) = \alpha_1 i\eta A_P S_a^*(\tau), \quad (7)$$

$$\frac{dS_a(\tau)}{d\tau} = -\Gamma_a S_a(\tau) + \alpha_2 i\eta A_P A_S^*(\tau), \quad (8)$$

where α_1, α_2 are some constants independent of ζ, τ . The two spatial equations in Eqs. (5) and (6) determine the shape of the spatial modes. Eliminating $A_S(\tau)$ in the two temporal equations in Eqs. (7) and (8), we have

$$\frac{dS_a}{d\tau} = (-\Gamma_a + l|\eta A_P|^2/c)S_a, \quad (9)$$

where $l/c \equiv \alpha_1^*\alpha_2$ defines an interaction length l , which is determined from the mode structure functions $\varphi(\zeta), \psi(\zeta)$. Oscillation for the atomic spin wave occurs when

$$-\Gamma_a + l|\eta A_P|^2/c \geq 0 \quad (10)$$

with the equality corresponding to the threshold. Notice that the loss of the Stokes field does not appear in the expression

above. This indicates that the role played by the Stokes field is not major but only supportive.

From the coupling coefficient in Eqs. (1) and (2), we have the threshold power for the Raman pump field

$$P_{th} \propto |A_P|^2 = c\Gamma_a/\eta^2 l \propto \Delta^2/N_a g_{eg}^2 g_{em}^2 \tau_c l. \quad (11)$$

where τ_c is the decoherence time for the atomic spin wave amplitude and is related to the decay constant by $\Gamma_a = 1/\tau_c$. From Ref. [41], we know $g_{em}, g_{eg} \propto V^{-1/2}$ with V as the volume of the interaction area of the Raman pump field and atoms. But $N_a = \rho V$ with ρ as the atomic density. If we let r be the waist of the Raman pump beam and L the interaction length, then $V = \pi r^2 L$. The threshold power can be written as

$$P_{th} \propto \Delta^2 V/\rho \tau_c \propto r^2 \Delta^2/\rho \tau_c. \quad (12)$$

IV. EXPERIMENTAL COMPARISON TO THE THEORY

The threshold power of the laserlike oscillation in Raman process in an atomic ensemble is then related to Δ, ρ, r , and τ_c . We will confirm experimentally this dependence next. Both the decoherence time τ_c and the atomic density ρ depend on the temperature of the cell with a more complicated dependence for ρ . In order to simplify the experiment, the temperature of the cell is fixed during the whole experiment at 68 °C.

First, we measure the threshold power P_{th} as a function of the frequency detuning. From Fig. 2, we find that the value of P_{th} can be extracted as the x -axis intercept. This is usually done by measuring the Stokes field or the anti-Stokes output as a function of the power of the pump field. During the measurement period, detuning Δ should be held constant. However, for a free-running laser, it is hard to hold frequency steady for long. Furthermore, there is also an issue of determining the detuning accurately. So, instead of holding the detuning constant, we scan the detuning by tuning the laser frequency across the absorption spectrum of the ^{87}Rb atoms while holding the Raman pump power constant. In the meanwhile, we record the intensities of the Stokes and anti-Stokes fields together with the the absorption spectrum of Rb for calibration. We do this for a number of measurements of Raman pump power ranging from a few hundred microwatts to a few milliwatts. Since we record the laser frequency scanning ramp voltage, the Stokes intensity, the anti-Stokes intensity, and the absorption spectrum simultaneously for a specific Raman pump power, we thus can find the Stokes and the anti-Stokes intensity for a certain pump power at a fixed detuning. From the graph of the output intensities versus the pump power as in Fig. 2, we can extract the threshold pump power for a specific detuning.

In Fig. 3 we plot the threshold power P_{th} as a function of the frequency detuning Δ . The P_{th} monotonically increases with Δ experimentally when Δ is larger than 0.3 GHz (region III) and smaller than -1.1 GHz (region I) but behaves in a complicated manner between -1.1 and 0.3 GHz (region II). In Fig. 3 the Doppler absorption spectrum (DAS) of the Rb atoms with mixed isotopes is also given as a reference for frequency calibration. There are two absorption dips, P_1 and P_2 , in DAS, corresponding to the transitions from $|g\rangle$ to $|5^2P_{1/2}, F=1\rangle$ and $|5^2P_{1/2}, F=2\rangle$ of ^{87}Rb (the larger absorption dip on the

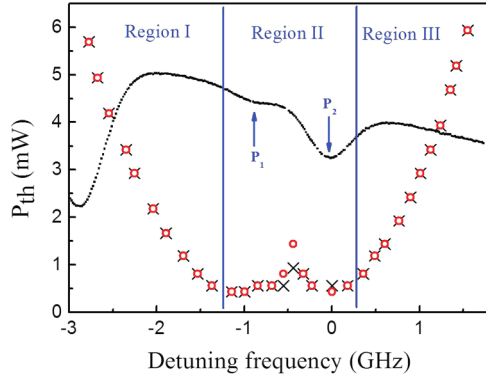


FIG. 3. (Color online) The threshold power of the Raman pump P_{th} as a function of the detuning frequency Δ of the pump laser from $|e_2\rangle$. Red circle: Experimental data of anti-Stokes field; black cross: experimental data of Stokes field; black solid line: absorption spectrum of Rb (mixed isotopes) for frequency calibration.

left is from ^{85}Rb and is irrelevant here because we use pure ^{87}Rb . The frequency difference between $|5^2P_{1/2}, F=1\rangle$ and $|5^2P_{1/2}, F=2\rangle$ is 0.8 GHz. The full width at half maximum of a single Doppler peak at a cell temperature of 68°C is about 0.7 GHz. So there is about a 1.4 GHz overlap region between the two dips.

The formula for the threshold power [Eq. (12)] in the theory discussed earlier is for the case with one excited state ($|e\rangle$). But we have two excited states here. To better analyze the data, we divide the whole frequency detuning region of the Raman pump field into three parts as shown in Fig. 3. In regions I and III, the Raman pump field is closer to one of the two excited states than the other, and the contribution from the farther states is small and can be approximately negligible. So we can still use Eq. (12) to fit the data. This is the reason why P_{th} monotonically increases with Δ . But in region II, the Raman scattering on $|5^2P_{1/2}, F=1, 2\rangle$ levels influence each other; the complicated behavior of P_{th} in region II in experiment is caused by the cross-influence of the two excited levels and the loss of the Stokes field close to resonance. Notice that the values of P_{th} are the smallest around the region close to resonance even though the loss of the Stokes field is the largest. This indicates that the effect of the loss of the Stokes field is small, in agreement with what we claimed earlier Eq. (10).

P_{th} in region I as a function of $(\Delta + 0.8)^2$ is given in Fig. 4(a), and P_{th} in region III as a function of Δ^2 is given in Fig. 4(b). The offset of 0.8 GHz in frequency for the data in region I is because the resonance line is P_1 , which is 0.8 GHz from $\Delta = 0$. The blue line is the linear fit to the experimental result, which shows that the threshold power of the Raman pump field P_{th} for the onset of the laserlike oscillation in Raman process is proportional to the square of the frequency detuning Δ^2 . The experimental results agree well with the theory in the Eq. (12).

In Eq. (12), besides the detuning frequency, the threshold power also depends on the waist r and the decoherence time τ_c of the atomic spin wave. But we know that the intensity is related to the power by $I = P/\pi r^2$. So Eq. (12) is changed to

$$I_{th} = P_{th}/\pi r^2 \propto \Delta^2/\tau_c. \quad (13)$$

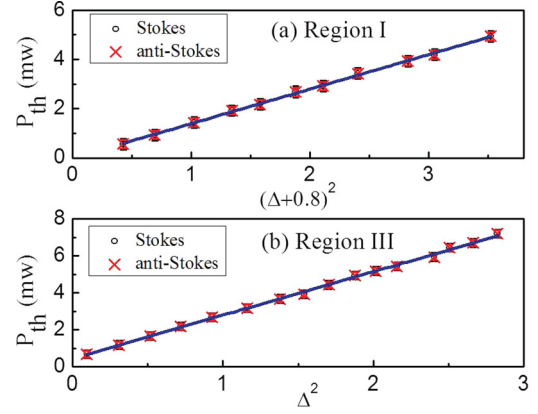


FIG. 4. (Color online) The threshold power of the Raman pump as a function of the square of frequency detuning. (a) Region I, $(\Delta + 0.8)$ is the value of the detuning frequency from $5^2P_{1/2}, F=1$ energy level. (b) Region III, Δ is the value of the detuning frequency from $5^2P_{1/2}, F=2$ energy level.

Hence, the threshold intensity is inversely proportional to the decoherence time.

Next, we investigate experimentally the τ_c dependence of the threshold power as predicted in Eq. (13). For the hyperfine splitting ground state of ^{87}Rb , the upper state is a metastable state having an extremely long decay time. However, for atoms in a hot vapor cell, the atomic motion will bring the atoms out of the interaction region with the light field, resulting in a loss for the atomic spin wave. So the decoherence time of the atomic coherence in vapor cell is approximately determined by the time that the atom flies out of the region of the Raman pump beam, i.e., $\tau_c = r/v_a$ with r as the waist of the pump field and v_a as the average speed of the atoms. For ^{87}Rb at 68°C , we obtain $v_a = 400$ m/s so that the decoherence time τ_c can be calculated from the waist of the pump field. Let us rewrite Eq. (13) as

$$\log_{10}(I_{th}/\Delta^2) = -\log_{10}(\tau_c) + C_0, \quad (14)$$

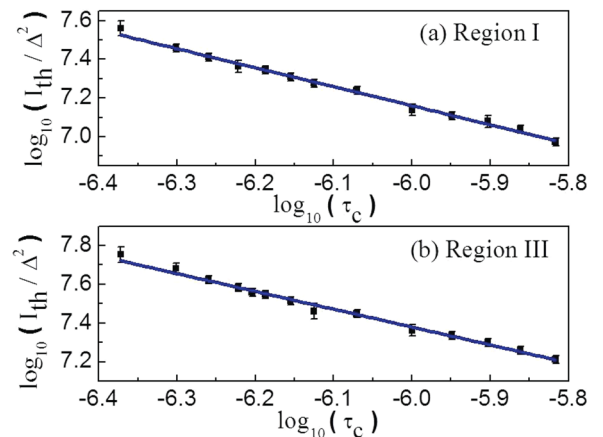


FIG. 5. (Color online) The logarithms of threshold intensity of the Raman pump as a function of the logarithms of the decoherence time τ_c (in μs). The black dot represents experimental result and the blue line is a linear fit.

where C_0 is some constant. In our experiment, P_{th}/Δ^2 can be extracted as the slope of the linear fit result in Fig. 4(a) and 4(b). When the waist is changed from 0.17 to 0.61 mm, a set of the P_{th}/Δ^2 or I_{th}/Δ^2 values can be obtained. The logarithm of I_{th}/Δ^2 as a function of the logarithm of the decoherence time τ_c is shown in Fig. 5. We linearly fit the experimental data in Fig. 5(a) and 5(b). The slopes of the linear fit are found to be -0.99 and -1.05 in regions I and III, respectively, which agree well with the prediction in Eq. (14).

V. SUMMARY AND DISCUSSION

In summary, we demonstrated a mirrorless laserlike oscillation of atomic spin waves in Raman process in a ^{87}Rb vapor cell. We used a simple theory of three-wave mixing to describe the phenomenon and found that the onset of the oscillation relies on a coherent buildup of the atomic spin wave. The simple theory predicts that the oscillation threshold intensity depends on atomic coherence time and the coupling efficiency between light and the atomic ensemble. This is verified experimentally. The observed threshold does not depend on the loss of the Stokes field in the system, indicating that it is not the buildup of the Stokes field that leads to the oscillation, as in most of the phenomena in mirrorless laser oscillation such as superfluorescence and amplified spontaneous emission.

The coherent buildup of the atomic spin wave here is similar to the on-resonance condition of the idler field in an optical parametric oscillator or a singly resonant optical parametric oscillator. Indeed, we can derive the exact formula for the threshold in Eq. (10) from the theory for a singly resonant optical parametric oscillator [42] after assigning proper quantities for losses and reflectivity.

Our atomic cell system has a quite long decoherence time (on the order of microseconds) for the atomic spin wave, which is orders of magnitude as large as those (on the order of picoseconds) in Raman processes in other media. This together with the near-resonance condition ($\Delta \ll \omega_P$) leads to an extremely low threshold (on the order of a few hundred microwatts) for the onset of the oscillation as compared to Raman processes in other media (on the order of megawatts).

ACKNOWLEDGMENTS

This work was supported by the National Basic Research Program of China (973 Program Grant No. 2011CB921604), the National Natural Science Foundation of China (Grant Nos. 11004058, 11004059, 11129402, 11274118, and 11234003), and the Innovation Program of Shanghai Municipal Education Commission 13zz036, the fundamental research funds for the central universities.

-
- [1] E. J. Woodbury and W. K. Ng, *Proc. IRE* **50**, 2347 (1962).
 - [2] R. W. Hellwarth, *Phys. Rev.* **130**, 1850 (1963).
 - [3] J. B. Grun, A. K. McGuillan, and B. P. Stoicheff, *Phys. Rev.* **180**, 61 (1969).
 - [4] Y. R. Shen and Y. J. Shaham, *Phys. Rev.* **163**, 224 (1967).
 - [5] Y. R. Shen, *The Principles of Nonlinear Optics* (John Wiley & Sons, New York, 1984).
 - [6] L. M. Duan, M. D. Lukin, J. I. Cirac, and P. Zoller, *Nature (London)* **414**, 413 (2001).
 - [7] R. Chrapkiewicz and W. Wasilewski, *Opt. Express* **20**, 29540 (2012).
 - [8] J. Kołodziej, J. Chwedeńczuk, and W. Wasilewski, *Phys. Rev. A* **86**, 013818 (2012).
 - [9] M. Fleischhauer and M. D. Lukin, *Phys. Rev. Lett.* **84**, 5094 (2000).
 - [10] C. Liu, Z. Dutton, C. H. Behroozi, and L. V. Hau, *Nature (London)* **409**, 490 (2001).
 - [11] D. F. Phillips, A. Fleischhauer, A. Mair, R. L. Walsworth, and M. D. Lukin, *Phys. Rev. Lett.* **86**, 783 (2001).
 - [12] A. V. Turukhin, V. S. Sudarshanam, M. S. Shahriar, J. A. Musser, B. S. Ham, and P. R. Hemmer, *Phys. Rev. Lett.* **88**, 023602 (2001).
 - [13] K. F. Reim, J. Nunn, V. O. Lorenz, B. J. Sussman, K. C. Lee, N. K. Langford, D. Jaksch, and I. A. Walmsley, *Nature Photon.* **4**, 218 (2010).
 - [14] K. F. Reim, P. Michelberger, K. C. Lee, J. Nunn, N. K. Langford, and I. A. Walmsley, *Phys. Rev. Lett.* **107**, 053603 (2011).
 - [15] A. Kuzmich, W. P. Bowen, A. D. Boozer, A. Boca, C. W. Chou, L.-M. Duan, and H. J. Kimble, *Nature (London)* **423**, 731 (2003).
 - [16] C. H. van der Wal, M. D. Eisaman, A. André, R. L. Walsworth, D. F. Phillips, A. S. Zibrov, and M. D. Lukin, *Science* **301**, 196 (2003).
 - [17] Z. Y. Ou, *Phys. Rev. A* **78**, 023819 (2008).
 - [18] W. Wasilewski and M. G. Raymer, *Phys. Rev. A* **73**, 063816 (2006).
 - [19] M. D. Eisaman, L. Childress, A. André, F. Massou, A. S. Zibrov, and M. D. Lukin, *Phys. Rev. Lett.* **93**, 233602 (2004).
 - [20] M. Jain, H. Xia, G. Y. Yin, A. J. Merriam, and S. E. Harris, *Phys. Rev. Lett.* **77**, 4326 (1996).
 - [21] A. J. Merriam, S. J. Sharpe, M. Shverdin, D. Manuszak, G. Y. Yin, and S. E. Harris, *Phys. Rev. Lett.* **84**, 5308 (2000).
 - [22] L. Q. Chen, G. W. Zhang, C. H. Yuan, J. Jing, Z. Y. Ou, and W. P. Zhang, *Appl. Phys. Lett.* **95**, 041115 (2009).
 - [23] C. H. Yuan, L. Q. Chen, J. Jing, Z. Y. Ou, and W. P. Zhang, *Phys. Rev. A* **82**, 013817 (2010).
 - [24] B. Chen, K. Zhang, C. Bian, C. Qiu, C.-H. Yuan, L. Q. Chen, Z. Y. Ou, and W. Zhang, *Opt. Express* **21**, 10490 (2013).
 - [25] L. Q. Chen, G.-W. Zhang, C.-L. Bian, C.-H. Yuan, Z. Y. Ou, and W. Zhang, *Phys. Rev. Lett.* **105**, 133603 (2010).
 - [26] L.-Q. Chen, C.-L. Bian, G.-W. Zhang, Z. Y. Ou, and W. Zhang, *Phys. Rev. A* **82**, 033832 (2010).
 - [27] D. Felinto, C. W. Chou, H. de Riedmatten, S. V. Polyakov, and H. J. Kimble, *Phys. Rev. A* **72**, 053809 (2005).
 - [28] D. M. Harber, H. J. Lewandowski, J. M. McGuirk, and E. A. Cornell, *Phys. Rev. A* **66**, 053616 (2002).
 - [29] P. Treutlein, P. Hommelhoff, T. Steinmetz, T. W. Hänsch, and J. Reichel, *Phys. Rev. Lett.* **92**, 203005 (2004).
 - [30] M. Uchida, K. Nagasaka, and H. Tashiro, *Opt. Lett.* **14**, 1350 (1989).

- [31] R. H. Stolen, E. P. Ippen, and A. R. Tynes, *Appl. Phys. Lett.* **20**, 62 (1972).
- [32] E. P. Ippen, *Appl. Phys. Lett.* **16**, 303 (1970).
- [33] S. E. Harris, *Appl. Phys. Lett.* **9**, 114 (1966).
- [34] A. S. Zibrov, M. D. Lukin, and M. O. Scully, *Phys. Rev. Lett.* **83**, 4049 (1999).
- [35] R. H. Dicke, *Phys. Rev.* **93**, 99 (1954).
- [36] R. Bonifacio and L. A. Lugiato, *Phys. Rev. A* **11**, 1507 (1975).
- [37] F. Auzel, S. Hubert, and D. Meichenin, *Europhys. Lett.* **7**, 459 (1988).
- [38] M. G. Raymer, Z. W. Li, and I. A. Walmsley, *Phys. Rev. Lett.* **63**, 1586 (1989).
- [39] M. G. Raymer and J. Mostowski, *Phys. Rev. A* **24**, 1980 (1981).
- [40] C. H. Yuan, L. Q. Chen, Z. Y. Ou, and W. P. Zhang, *Phys. Rev. A* **87**, 053835 (2013).
- [41] M. O. Scully and M. S. Zubairy, *Quantum Optics* (Cambridge University Press, New York, 1997).
- [42] A. Yariv, *Quantum Electronics* (John Wiley & Sons, New York, 1989).